

# QED on the lattice and numerical perturbative computation of $g - 2$

---

Ryuichiro Kitano<sup>1,2</sup>, Hiromasa Takaura<sup>1</sup>

<sup>1</sup>*KEK Theory Center, Tsukuba 305-0801, Japan*

<sup>2</sup>*Graduate University for Advanced Studies (Sokendai), Tsukuba 305-0801, Japan*

*E-mail:* [ryuichiro.kitano@kek.jp](mailto:ryuichiro.kitano@kek.jp), [htakaura@post.kek.jp](mailto:htakaura@post.kek.jp)

ABSTRACT: We compute the electron  $g$  factor to the  $\mathcal{O}(\alpha^5)$  order on the lattice in quenched QED. We first study finite volume corrections in various IR regularization methods to discuss which regularization is optimal for our purpose. We point out that finite volume corrections in QED<sub>L</sub> and QED<sub>TL</sub> cannot be obtained correctly when an external momentum of correlation functions is set to on-shell from the beginning as previous studies do. We adopt finite photon mass regularization to suppress finite volume effects exponentially and also discuss our strategy about choice of simulation parameters and the order of extrapolations to efficiently obtain the  $g$  factor. We perform lattice simulation using small lattices to test feasibility of our calculation strategy. This study can be regarded as an intermediate step toward giving the five-loop coefficient independently of the preceding studies.

---

## Contents

<b>1</b>	<b>Introduction</b>	<b>1</b>
<b>2</b>	<b>Finite volume corrections in lattice QED</b>	<b>2</b>
2.1	QED <sub>L</sub> and QED <sub>TL</sub> for $p = (0, 0, 0, p_4)$	4
2.2	Modified QED <sub>L</sub> for $p = (0, 0, p_3, p_4)$	6
2.3	Massive photon regularization	9
<b>3</b>	<b>Lattice calculation of <math>g - 2</math></b>	<b>9</b>
3.1	Outline of the method	10
3.2	Backward propagation and its suppression	12
3.3	Effects of $m_\gamma$ , $k^2$ , and $\Lambda_{\text{UV}}^2$	13
3.4	Calculation strategy	14
3.5	Numerical results	15
<b>4</b>	<b>Conclusions and discussion</b>	<b>19</b>

---

## 1 Introduction

The anomalous magnetic moment of the electron, the electron  $g - 2$ , is one of the most precisely measured observables in particle physics. It thus gives us a good opportunity to test our understanding of quantum field theory. Theoretically the perturbative calculation of QED contributions has reached the five-loop [ $\mathcal{O}(\alpha^5)$ ] level [1], although a slight discrepancy in the five-loop coefficient is reported [2]. The current theoretical prediction fairly agrees well with the experimental result [3–5], whose precision is actually sensitive to the five-loop result. In order to thoroughly examine the consistency of the SM prediction with the experimental result, the value of the fine structure constant seems crucial, yet the value is not determined consistently among different experiments [6].

In ref. [7], we proposed a new method to calculate the perturbative series of the electron  $g - 2$  using numerical stochastic perturbation theory (NSPT) [8–12]. We calculated the perturbative series to the three-loop level on small lattices. This was the first attempt to apply NSPT to QED observables. Since it can provide us with a new and alternative approach to calculating the perturbative series to high orders and can have a wide range of application, it is worth testing the usefulness of the method further.

In order to perform meaningful numerical simulations, we need to understand finite volume (FV) corrections, which are known to be severe in lattice QED because of massless photon. In this paper, we study FV corrections in various ways of IR regularization such as subtractions of zero modes and finite photon mass [13–15] to understand what kind of

IR regularization is optimal, although FV corrections are not understood enough in our previous work [7]. We also correct a result for FV corrections obtained in ref. [16].

In this paper, we perform lattice simulation of the electron  $g - 2$  in quenched QED, i.e., QED without the dynamical electron. We adopt finite photon mass regularization. In quenched QED, i.e., in sub-diagrams without lepton loops, there is discrepancy in the five-loop perturbative coefficient between refs. [3, 17] and ref. [2]. Our study can potentially give an independent result. As an attempt, we perform a five-loop level calculation on the lattice. Our present study does not quite give a conclusive result due to small lattice sizes. We regard the study in this paper as an intermediate step toward obtaining the continuum limit result of the five-loop coefficient.

The achievements of the present paper can be stated as follows. First, the higher order calculation than our previous study [7] is made possible. This is because we use a method to suppress backward propagations, which are a serious obstacle in the analysis in ref. [7]. The higher order calculation can be done also because numerical costs to generate configurations are drastically reduced due to quenched QED. In quenched QED, interaction terms are absent and the Langevin equation becomes trivial. Therefore, configurations are generated according to Gaussian distribution. In this sense, the present paper tests efficiency of numerical calculation of perturbative series in lattice rather than NSPT itself. Secondly, we discuss in detail the strategy for the choice of simulation parameters and also the order of various extrapolations. This is based on understanding of systematic errors such as FV corrections, finite photon mass effects, which are studied in this paper.

The paper is organized as follows. In Sec. 2, we study FV corrections in various IR regularization method to discuss what kind of IR regularization we should adopt. In Sec. 3, we perform a lattice simulation. We first explain the outline of our calculation, and then we study systematic uncertainties of our calculation to discuss the strategy about choice of simulation parameters and the order of various extrapolations. Then we perform our numerical simulation following the strategy to examine its feasibility. Sec. 4 is devoted to the conclusions and discussion.

## 2 Finite volume corrections in lattice QED

Before we try to calculate any physical quantities in QED, we should first give a concrete definition of QED. Especially, in a finite volume, the infrared divergence needs to be carefully treated in order to make a prediction which coincides with QED in continuum and infinite volume spacetime as a certain limit. We below discuss and compare various definitions proposed or used in the literature. We will see that the regularization by finite photon mass is the best controlled method for our  $g - 2$  computations.

We consider FV effects in various IR regularization methods:  $\text{QED}_L$ ,  $\text{QED}_{TL}$ , an extension of  $\text{QED}_L$ , and massive photon regularization [13–15]. The precise meaning of these regularizations is explained below. Although  $\text{QED}_L$  and  $\text{QED}_{TL}$  are famous regularizations of lattice QED, we point out that previous study of FV corrections is not always correct.

We consider the following quantity as an example:

$$I = \not\int \frac{1}{k^2 + m_\gamma^2} \frac{1}{(k+p)^2 + m^2}. \quad (2.1)$$

Here  $k$  denotes loop momentum and  $p$  external momentum. The summation/integral symbol represents the sum/integration of the loop momentum  $k$ , and its precise meaning depends on regularization schemes as discussed below. The above quantity mimics the two-point function in scalar QED.  $m_\gamma$  denotes photon mass, which will be set to zero or non-zero below. In lattice QED, the zero mode of loop momentum  $k = (0, 0, 0, 0)$  makes the result diverge. Therefore some regularization of the zero mode is needed. One way is to introduce non-zero photon mass. There are alternative methods which do not introduce photon mass but modify the range of loop momentum sum. QED<sub>L</sub> and QED<sub>TL</sub> define  $\not\int$  as follows:

$$\begin{aligned} \text{QED}_L \text{ on } \mathbb{T}^3 \times \mathbb{R} : \quad \not\int &= \frac{1}{L^3} \sum_{\vec{k} \in B\mathbb{Z}_L^3 \setminus \{0\}} \int \frac{dk_4}{2\pi}, \\ \text{QED}_L \text{ on } \mathbb{T}^4 : \quad \not\int &= \frac{1}{L^3 T} \sum_{k_4 \in B\mathbb{Z}_T} \sum_{\vec{k} \in B\mathbb{Z}_L^3 \setminus \{0\}}, \\ \text{QED}_{TL} \text{ on } \mathbb{T}^4 : \quad \not\int &= \frac{1}{L^3 T} \sum_{k \in B\mathbb{Z}_{TL}^4 \setminus \{0\}}, \end{aligned} \quad (2.2)$$

where  $\vec{k} = (k_1, k_2, k_3)$ ,  $B\mathbb{Z}_L = \frac{2\pi}{L}\mathbb{Z} = \{\frac{2\pi}{L}n | n \in \mathbb{Z}\}$ ,  $B\mathbb{Z}_T = \frac{2\pi}{T}\mathbb{Z}$ ,  $B\mathbb{Z}_{TL}^4 = B\mathbb{Z}_L^3 \times B\mathbb{Z}_T$ , and  $\setminus \{0\}$  means removal of the element  $(0, \dots, 0)$ . In these regularization methods, the photon mass is set to zero. We note that, although  $\mathbb{T}^3 \times \mathbb{R}$  cannot be realized in actual lattice simulations, it is convenient to consider QED<sub>L</sub> on  $\mathbb{T}^3 \times \mathbb{R}$  as an intermediate step for clarifying the difference between QED on  $\mathbb{R}^4$  and an above theory, as explained in ref. [16]. In other words, we can clarify FV corrections of, for instance, QED<sub>L</sub> on  $\mathbb{T}^4$ , considering the chain (QED on  $\mathbb{R}^4$ )  $\rightarrow$  (QED<sub>L</sub> on  $\mathbb{T}^3 \times \mathbb{R}$ )  $\rightarrow$  (QED<sub>L</sub> on  $\mathbb{T}^4$ ) and studying the difference of each deformation.

In Sec. 2.1, we study FV corrections in QED<sub>L</sub> and QED<sub>TL</sub> for external momentum  $p = (0, 0, 0, p_4)$ , where only the fourth component is non-zero. This momentum choice is relevant to mass measurement because masses can be extracted from a two-point function whose sources are separated only in time direction. In our study, we do not set the external momentum to on shell  $p_4 = im$  from the beginning unlike previous works and we consider general Euclidean momentum. In Sec. 2.2, we study FV corrections in modified QED<sub>L</sub> and QED<sub>TL</sub> for external momentum  $p = (0, 0, p_3, p_4)$ . The reason why we also study this case is that multiple non-zero components are necessary to extract magnetic form factor. (To extract magnetic form factor, of course, we have to consider a three-point function, but it is more difficult to analyze and our study for the two-point function is already suggestive.) This momentum choice requires modification of QED<sub>L</sub> and QED<sub>TL</sub>. In Sec. 2.3, we study FV corrections in massive photon theory. In this case, there is no need to specify external momentum.

## 2.1 QED<sub>L</sub> and QED<sub>TL</sub> for $p = (0, 0, 0, p_4)$

We study FV corrections in QED<sub>L</sub> and QED<sub>TL</sub> setting  $p = (0, 0, 0, p_4)$ . We can study them by considering a sequence of deformation, (QED on  $\mathbb{R}^4$ )  $\rightarrow$  (QED<sub>L</sub> on  $\mathbb{T}^3 \times \mathbb{R}$ )  $\rightarrow$  (QED<sub>L</sub> on  $\mathbb{T}^4$ )  $\rightarrow$  (QED<sub>TL</sub> on  $\mathbb{T}^4$ ).

**QED on  $\mathbb{R}^4 \rightarrow$  QED<sub>L</sub> on  $\mathbb{T}^3 \times \mathbb{R}$**

First we consider the difference between QED<sub>L</sub> on  $\mathbb{T}^3 \times \mathbb{R}$  and QED on  $\mathbb{R}^4$ . It is given by [13]

$$\begin{aligned} \Delta I(L) &\equiv \left( \sum_{\text{QED on } \mathbb{R}^4} - \sum_{\text{QED}_L \text{ on } \mathbb{T}^3 \times \mathbb{R}} \right) \frac{1}{k^2} \frac{1}{(k+p)^2 + m^2} \\ &= - \left( \sum_{\vec{x} \in L\mathbb{Z}^3 \setminus \{0\}} - \frac{1}{L^3} \int d^3x \right) \int \frac{d^4k}{(2\pi)^4} \frac{1}{k^2} \frac{1}{(k+p)^2 + m^2} e^{i\vec{k} \cdot \vec{x}} \\ &= - \frac{1}{(4\pi)^2} \int_0^1 dy \int_0^\infty ds s^{-1} e^{-\frac{s}{4\pi}[y(1-y)p^2 + ym^2]L^2} \left( \vartheta_3(0, e^{-\pi/s})^3 - 1 - s^{3/2} \right). \end{aligned} \quad (2.3)$$

Here we used the Poisson resummation to rewrite the KK sum by integrations and  $L\mathbb{Z} = \{Ln | n \in \mathbb{Z}\}$ .  $\int d^3x$  corresponds to the subtraction of the spatial zero mode (since it gives  $(2\pi)^3 \delta^3(\vec{k})$ ) and we rewrote the propagators by the Feynman parameter ( $y$ ) integral and performed the momentum integration.  $\vartheta_3$  denotes the elliptic theta function,  $\vartheta_3(0, e^{-\pi/s}) = \sum_{n=-\infty}^{\infty} e^{-\pi n^2/s}$ .

To study the asymptotic form of  $\Delta I$  for  $L \rightarrow \infty$ , we consider

$$\widetilde{\Delta I}(u) \equiv \int_0^\infty dL L^{-u-1} \Delta I(L). \quad (2.4)$$

We can see the asymptotic behavior of  $\Delta I$  by studying singularities of this function. If  $\Delta I$  behaves as  $\Delta I \sim L^{-u_0}$  for  $L \gg 1$ ,  $\widetilde{\Delta I}(u)$  develops singularities at  $u = -u_0$  due to a divergence of the integral of eq. (2.4) around  $L \sim \infty$ .

We obtain

$$\begin{aligned} \widetilde{\Delta I}(u) &= - \frac{1}{32\pi^2} \frac{1}{(4\pi)^{u/2}} \Gamma(-u/2) \int_0^1 dy [y(1-y)p^2 + ym^2]^{u/2} \\ &\quad \times \int_0^\infty ds s^{u/2-1} \left( \vartheta_3(0, e^{-\pi/s})^3 - 1 - s^{3/2} \right). \end{aligned} \quad (2.5)$$

The  $y$ -integral and the  $s$ -integral are factorized. The first singularity of  $\widetilde{\Delta I}(u)$  at negative  $u$  is located at  $u = -2$ , where the  $y$ -integral diverges. This tells us that the asymptotic behavior of  $\Delta I(L)$  is  $\Delta I(L) \sim L^{-2}$ . The  $s$ -integral is convergent for  $u = 2$ . To examine the convergence of the  $s$ -integral, it is convenient to keep the following relation in mind:

$$\vartheta_3(0, e^{-\pi/s}) = \sum_{n=-\infty}^{\infty} e^{-\frac{\pi}{s}n^2} = \sum_{m=-\infty}^{\infty} \int \frac{dk}{2\pi} e^{-\frac{k^2}{4\pi s}} e^{ikm} = s^{1/2} \sum_{m=-\infty}^{\infty} e^{-\pi sm^2} = s^{1/2} \vartheta_3(0, e^{-\pi s}), \quad (2.6)$$

where we used the Poisson resummation in the first equality and then performed the Gaussian integral. Thus one can see that

$$\begin{aligned} \vartheta_3(0, e^{-\pi/s})^3 - 1 &\sim (1 + 2e^{-\pi/s})^3 - 1 && \text{for } s \ll 1 \\ \vartheta_3(0, e^{-\pi/s})^3 - s^{3/2} &\sim [s^{1/2}(1 + 2e^{-s\pi})]^3 - s^{3/2} && \text{for } s \gg 1 \end{aligned} \quad (2.7)$$

are very suppressed functions. The expansion of  $\widetilde{\Delta I}(u)$  around  $u = -2$  is given by

$$\widetilde{\Delta I}(u) = -\frac{\kappa_{-2}}{4\pi} \frac{1}{p^2 + m^2} \frac{1}{u + 2} + \mathcal{O}((u + 2)^0), \quad (2.8)$$

where

$$\kappa_{-2} \equiv \int_0^\infty ds s^{-2} \left( \vartheta_3(0, e^{-\pi/s})^3 - 1 - s^{3/2} \right) \simeq -2.837. \quad (2.9)$$

The inverted formula of eq. (2.4) is given by

$$\Delta I(L) = \frac{1}{2\pi i} \int_{-i\infty}^{i\infty} du L^u \widetilde{\Delta I}(u). \quad (2.10)$$

Calculating eq. (2.10) by changing the integration path  $-i\infty \rightarrow i\infty$  to the contour surrounding the pole at  $u = -2$ , we obtain

$$\Delta I(L) = -\frac{\kappa_{-2}}{4\pi} \frac{1}{p^2 + m^2} \frac{1}{L^2} + (\text{higher order in } 1/L). \quad (2.11)$$

We note that *the FV correction is singular at the on-shell momentum.*

**QED<sub>L</sub> on  $\mathbb{T}^3 \times \mathbb{R} \rightarrow$  QED<sub>L</sub> on  $\mathbb{T}^4$**

Next we consider the difference between QED<sub>L</sub> on  $\mathbb{T}^3 \times \mathbb{R}$  and QED<sub>L</sub> on  $\mathbb{T}^4$ :

$$\begin{aligned} \Delta' I(L, T) &= \left( \sum_{\text{QED}_L \text{ on } \mathbb{T}^3 \times \mathbb{R}} - \sum_{\text{QED}_L \text{ on } \mathbb{T}^4} \right) \frac{1}{k^2} \frac{1}{(k+p)^2 + m^2} \\ &= -\frac{1}{L^3} \sum_{\vec{k} \in B\mathbb{Z}_L^3 \setminus \{0\}} \sum_{x_4 \in T\mathbb{Z} \setminus \{0\}} \int \frac{dk_4}{2\pi} \frac{1}{k^2} \frac{1}{(k+p)^2 + m^2} e^{ik_4 x_4} \\ &\sim e^{-|\vec{k}|_{\min} T} \sim e^{-2\pi \frac{T}{L}}. \end{aligned} \quad (2.12)$$

In the last line, we only showed the exponential factor of the contribution which is given by the possible smallest  $|\vec{k}|$  and  $|x_4|$ . ( $\int dk_4$  is performed by using the Cauchy theorem.)

**QED<sub>L</sub> on  $\mathbb{T}^4 \rightarrow$  QED<sub>TL</sub> on  $\mathbb{T}^4$**

The difference between QED<sub>L</sub> on  $\mathbb{T}^4$  and QED<sub>TL</sub> on  $\mathbb{T}^4$  is given by

$$\begin{aligned} \Delta'' I(L, T) &= \left( \sum_{\text{QED}_L \text{ on } \mathbb{T}^4} - \sum_{\text{QED}_{TL} \text{ on } \mathbb{T}^4} \right) \frac{1}{k^2} \frac{1}{(k+p)^2 + m^2} \\ &= -\frac{1}{L^3 T} \sum_{k_4 \in B\mathbb{Z}_T \setminus \{0\}} \frac{1}{k^2} \frac{1}{(k+p)^2 + m^2} \Big|_{\vec{k}=0} \\ &= -\frac{T}{L^3} \sum_{n \neq 0} \frac{1}{4\pi^2 n^2} \frac{1}{\left(\frac{2\pi n}{T} + p_4\right)^2 + m^2}. \end{aligned} \quad (2.13)$$

We may give a bound  $|\Delta''I| \leq \frac{T}{L^3} \frac{1}{m^2} \sum_{n \neq 0} \frac{1}{n^2}$ .

We are now ready to give FV corrections in QED<sub>L</sub> on  $\mathbb{T}^4$  and those in QED<sub>TL</sub> on  $\mathbb{T}^4$  using the above results. The FV corrections in QED<sub>L</sub> on  $\mathbb{T}^4$  is given by  $\Delta I + \Delta' I$ . For  $2\pi T/L \gg 1$ ,  $\Delta' I$  is exponentially suppressed and the FV corrections are solely given by  $\Delta I \sim 1/[L^2(p^2 + m^2)]$ .

Our result here corrects the previous result for the FV corrections obtained in ref. [16], where it is stated that the FV corrections in QED<sub>L</sub> of  $I$  are  $\sim 1/(mL)$ . This disagreement stems from the fact that they consider Minkowski momentum  $p_4 = im$  from the beginning while we consider Euclidean momentum. Indeed, if  $p^2 = -m^2$  is considered from the beginning, eq. (2.5) has a pole at  $u = -1$ , which shows that the FV corrections are  $\sim 1/(mL)$ . This modification can be understood from the fact that the IR behavior of the integrand of  $I$  gets severer for the on-shell momentum than Euclidean momentum. We infer that, in actual lattice simulations where mass is read off from Fourier transform of a Euclidean correlator, the FV effects are given by  $\mathcal{O}(1/L^2)$  from the following rough calculation.

$$\begin{aligned} & \int \frac{dp_4}{2\pi} \left[ \frac{1}{p^2 + m^2} + \frac{1}{p^2 + m^2} m^2 e^2 (I_\infty(p^2) + \Delta I(p^2)) \frac{1}{p^2 + m^2} \right] e^{ip_4 t} \\ &= \frac{1}{2m} e^{-mt} \left[ 1 + (1 + mt) e^2 \frac{I_\infty(p_4 = im)}{2} - e^2 \frac{\kappa-2}{4\pi} \frac{1}{8m^2 L^2} (3 + 3mt + m^2 t^2) \right] \\ &\simeq C \exp[-mt \left( 1 - e^2 \frac{I_\infty(p_4 = im)}{2} + e^2 \frac{\kappa-2}{4\pi} \frac{1}{8m^2 L^2} (3 + mt) \right)]. \end{aligned} \quad (2.14)$$

In the first expression, we added  $m^2$  in the numerator in order to compensate mass dimension, which is a very rough prescription.  $I_\infty(p^2)$  corresponds to the one-loop calculation in infinite volume spacetime and does not exhibit a pole at  $p^2 = -m^2$ . Here  $e^2 \frac{\kappa-2}{4\pi} \frac{1}{8m^2 L^2} (3 + mt)$  in the last expression denotes the FV correction factor to the mass, where explicit numbers are not important and only the functional form would be suggestive. This (very rough) calculation indicates that the FV correction is  $\mathcal{O}(1/(mL)^2)$  instead of  $\mathcal{O}(1/(mL))$ .

We also emphasize that neglecting  $\Delta' I$  in the FV corrections is justified when  $2\pi T/L \gg 1$ . Although practically this condition is usually satisfied, one should note that  $T \rightarrow \infty$  limit should be taken before  $L \rightarrow \infty$  in order to formally regard the FV corrections in QED<sub>L</sub> on  $\mathbb{T}^4$  as  $\Delta I$ .

The FV corrections to QED<sub>TL</sub> are given by  $\Delta I + \Delta' I + \Delta'' I$ . Due to  $\Delta'' I \sim T/L^3$ , the limit of  $T \rightarrow \infty$  should not be taken before  $L \rightarrow \infty$ . This was mentioned in ref. [16]. Therefore,  $L \rightarrow \infty$  limit should be first considered. In this case, since  $\Delta' I$  is not suppressed exponentially one should not neglect  $\Delta' I$  as a part of the FV corrections. In this case (i.e.  $2\pi T/L \ll 1$ ), the asymptotic behavior of  $\Delta' I$  for  $L \gg 1$  should be made clear, although this is beyond the scope of this paper.

## 2.2 Modified QED<sub>L</sub> for $p = (0, 0, p_3, p_4)$

We now move on to the case where two components of the external momentum are non-zero,  $p = (0, 0, p_3, p_4)$ , as this situation is relevant to our calculation to obtain form factors.

Then we start with the difference between modified QED<sub>L</sub> on  $\mathbb{T}^2 \times \mathbb{R}^2$  and QED on  $\mathbb{R}^4$ .  $\mathbb{T}^2 \times \mathbb{R}^2$  means that the three- and four-direction extend infinitely while the other directions are compactified. We mean modified QED<sub>L</sub> by subtraction of modes  $k = (0, 0, k_3, k_4)$  for arbitrary  $k_3$  and  $k_4$ . This is a natural extension of QED<sub>L</sub> for this external momentum. Then the difference is given by

$$\begin{aligned}
\Delta I &\equiv \left( \not\sum_{\text{QED on } \mathbb{R}^4} - \not\sum_{\text{mod. QED}_L \text{ on } \mathbb{T}^2 \times \mathbb{R}^2} \right) \frac{1}{k^2} \frac{1}{(k+p)^2 + m^2} \\
&= - \left( \sum_{\vec{x} \in L\mathbb{Z}^2 \setminus \{0\}} - \frac{1}{L^2} \int d^2x \right) \int \frac{d^4k}{(2\pi)^4} \frac{1}{k^2} \frac{1}{(k+p)^2 + m^2} e^{i\vec{k} \cdot \vec{x}} \\
&= - \frac{1}{(4\pi)^2} \int_0^1 dy \int_0^\infty ds s^{-1} e^{-\frac{s}{4\pi} [y(1-y)p^2 + ym^2] L^2} \left( \vartheta_3(0, e^{-\pi/s})^2 - 1 - s \right). \quad (2.15)
\end{aligned}$$

In this case the vector  $\vec{x}$  is a two-component vector where one- and two-component can be non-zero. In a parallel manner to the previous calculation, we consider  $\widetilde{\Delta I}$ :

$$\begin{aligned}
\widetilde{\Delta I}(u) &= \int_0^\infty dL L^{-u-1} \Delta I(L) \\
&= - \frac{1}{32\pi^2} \frac{1}{(4\pi)^{u/2}} \Gamma(-u/2) \int_0^1 dy [y(1-y)p^2 + ym^2]^{u/2} \\
&\quad \times \int_0^\infty ds s^{u/2-1} \left( \vartheta_3(0, e^{-\pi/s})^2 - 1 - s \right). \quad (2.16)
\end{aligned}$$

Both  $y$ -integral and  $s$ -integral diverge at  $u = -2$ . As a result,  $u = -2$  is a double pole:

$$\widetilde{\Delta I}(u) = f_{-2}(p^2) \frac{1}{(u+2)^2} + f_{-1}(p^2) \frac{1}{u+2} + \mathcal{O}(u+2), \quad (2.17)$$

where  $f_{-2}(p^2)$  and  $f_{-1}(p^2)$  are functions of  $p^2$  and singular at on-shell momentum. Therefore,  $\Delta I$  is given by

$$\Delta I = f_{-2}(p^2) \frac{1}{L^2} \log L + f_{-1}(p^2) \frac{1}{L^2} + (\text{higher order in } 1/L). \quad (2.18)$$

Now we have  $1/L^2 \log L$  in addition to  $1/L^2$ .

In the actual lattice simulation where the number of the sites of direction 1 and 2 is finite, we have to consider the following additional correction (as in the previous calcula-

tion):

$$\begin{aligned}
& \Delta' I(L, T) \\
&= \left( \not\int_{\text{mod. QED}_L \text{ on } \mathbb{T}^2 \times \mathbb{R}^2} - \not\int_{\text{mod. QED}_L \text{ on } \mathbb{T}^4} \right) \frac{1}{k^2} \frac{1}{(k+p)^2 + m^2} \\
&= -\frac{1}{L^2} \sum_{\vec{k} \in B\mathbb{Z}^2 \setminus \{0\}} \sum_{(x_3, x_4) \in L_3\mathbb{Z} \times T\mathbb{Z} \setminus \{0\}} \int \frac{d^2 \tilde{k}}{(2\pi)^2} \frac{1}{k^2} \frac{1}{(k+p)^2 + m^2} e^{i\tilde{k} \cdot \tilde{x}} \\
&= -\frac{1}{L^2} \sum_{\vec{k} \in B\mathbb{Z}^2 \setminus \{0\}} \sum_{(x_3, x_4) \in L_3\mathbb{Z} \times T\mathbb{Z} \setminus \{0\}} \frac{1}{4\pi} \int_0^1 dy \int_0^\infty ds e^{-s(y(1-y)p^2 + ym^2 + \vec{k}^2 + \frac{\tilde{x}^2}{4s^2})} e^{-iy\tilde{p} \cdot \tilde{x}},
\end{aligned} \tag{2.19}$$

where  $\tilde{k} = (k_3, k_4)$  and  $\vec{k} = (k_1, k_2)$ .  $\tilde{x}$  is understood in a parallel manner. We obtain a bound for the summand as

$$\begin{aligned}
& \frac{1}{L^2} \left| \int_0^1 dy \int_0^\infty ds e^{-s(y(1-y)p^2 + ym^2 + \vec{k}^2 + \frac{\tilde{x}^2}{4s^2})} e^{iy\tilde{p} \cdot \tilde{x}} \right| \\
& \leq \frac{1}{L^2} \int_0^1 dy \int_0^\infty ds e^{-s(\vec{k}^2 + \frac{\tilde{x}^2}{4s^2})} < \text{const.} \times \frac{1}{L^2} \frac{|\tilde{x}|^{1/2}}{|\vec{k}|^{3/2}} e^{-|\vec{k}||\tilde{x}|}
\end{aligned} \tag{2.20}$$

Here we used  $\int_0^\infty ds e^{-s(\vec{k}^2 + \frac{|\tilde{x}|^2}{4s^2})} = \frac{|\tilde{x}|}{|\vec{k}|} K_1(|\vec{k}||\tilde{x}|)$ , where  $K_1$  denotes the modified Bessel function of second kind, and the fact that there is a constant such that  $K_1(z) < \text{const.} \times \frac{1}{\sqrt{z}} e^{-z}$  for a certain region  $z > z_0$ . We set the number of sites as  $(L_1, L_2, L_3, T) = (L, L, L_3, T)$ . The possible largest exponential factor is given by  $e^{-2\pi L_3/L}$  and  $e^{-2\pi T/L}$ .

The FV corrections in the modified QED<sub>L</sub> is given by  $\Delta I + \Delta' I$ . To make  $\Delta' I$  exponentially suppressed, we need  $2\pi L_3/L, 2\pi T/L \gg 1$ . This result tells us that the lattice length of the directions whose external momentum components are non-zero should be taken larger than the others.

If QED<sub>TL</sub>, where only  $k = (0, 0, 0, 0)$  is subtracted, is considered, we also should add

$$\begin{aligned}
\Delta'' I(L, T) &= \left( \not\int_{\text{mod. QED}_L \text{ on } \mathbb{T}^4} - \not\int_{\text{QED}_{TL} \text{ on } \mathbb{T}^4} \right) \frac{1}{k^2} \frac{1}{(k+p)^2 + m^2} \\
&= -\frac{1}{L^2 L_3 T} \sum_{(k_3, k_4) \in B\mathbb{Z}_T \times B\mathbb{Z}_{L_3} \setminus \{0\}} \frac{1}{k^2} \frac{1}{(k+p)^2 + m^2} \Big|_{\vec{k}=0} \\
&= -\frac{1}{L^2 L_3 T} \sum_{(n_3, n_4) \in \mathbb{Z}^2 \setminus \{0\}} \frac{1}{\left(\frac{2\pi n_3}{L_3}\right)^2 + \left(\frac{2\pi n_4}{T}\right)^2} \frac{1}{\left(\frac{2\pi n_3}{L_3} + p_3\right)^2 + \left(\frac{2\pi n_4}{T} + p_4\right)^2 + m^2}.
\end{aligned} \tag{2.21}$$

Studying the asymptotic behavior of this function is beyond the scope of this paper.

### 2.3 Massive photon regularization

We consider massive photon regularization with photon mass of  $m_\gamma L \gg 1$ . In this case, the FV effects are known to be exponentially suppressed. Let us see this explicitly for clarity.  $I$  is evaluated as

$$I = \frac{1}{16\pi^2} \sum_{x \in L\mathbb{Z}^3 \times T\mathbb{Z}} \int_0^1 dy \int_0^\infty ds s^{-1} \exp \left[ - \left\{ s[y(1-y)p^2 + ym^2 + (1-y)m_\gamma^2] + \frac{|x|^2}{4s} \right\} - iyp \cdot x \right]. \quad (2.22)$$

The FV effect,  $\Delta I$ , is given by the contributions where  $x \neq 0$ . We obtain a bound

$$\begin{aligned} & \left| \int_0^\infty ds s^{-1} \exp \left[ - \left\{ s[y(1-y)p^2 + ym^2 + (1-y)m_\gamma^2] + \frac{|x|^2}{4s} \right\} - iyp \cdot x \right] \right| \\ & \leq \int_0^\infty ds s^{-1} \exp \left[ - \left\{ sm_\gamma^2 + \frac{|x|^2}{4s} \right\} \right] = 2K_0(m_\gamma|x|) < \frac{C}{\sqrt{m_\gamma|x|}} \exp[-m_\gamma|x|]. \end{aligned} \quad (2.23)$$

There exists a constant  $C$  satisfying the above inequality. In the above calculation, we assumed  $m^2 > m_\gamma^2$ , so that  $ym^2 + (1-y)m_\gamma^2 \geq m_\gamma^2$ . Using the above bound, we can see that the FV effects are suppressed as  $\sim e^{-m_\gamma L}, e^{-m_\gamma T}$  by focusing on the smallest  $|x|$  contributions, which dominate  $\Delta I$ .

Therefore, as long as we take  $m_\gamma L, m_\gamma T \gg 1$ , we can safely neglect FV effects on Euclidean quantities. As can be seen from the above calculations, this is true independent of choices of the external momentum.

We saw in Secs. 2.1 and 2.2 that there are subtle issues about FV corrections in QED<sub>L</sub> and QED<sub>TL</sub>. FV corrections in these regularizations can change its asymptotic behavior depending on external momentum or by slight modification of the range of loop momentum sum. We then consider it difficult to correctly understand FV corrections to the three-point function we discuss below to obtain the  $g$  factor in these regularizations. (In addition, as the order of loop expansion is raised, the three-point function starts to contain IR divergences.) We will adopt finite photon mass regularization since we can expect exponential suppression of FV corrections for arbitrary correlation functions and arbitrary external momenta.

### 3 Lattice calculation of $g - 2$

In this section, we perform perturbative computation of the electron  $g$  factor in lattice. We adopt photon mass regularization. In Sec. 3.1, we explain the outline of our calculation of the  $g$  factor. In Sec. 3.2, we study backward propagation and propose a method to suppress its effects. In Sec. 3.3, we study corrections to the  $g$  factor caused by finite photon mass, finite photon momentum, and finite smearing parameter, which are introduced in our calculation (but should be finally sent to zero or infinity). In Sec. 3.4, we then discuss an optimal strategy for extracting the  $g$  factor based on our understanding of systematic errors. In Sec. 3.5, we carry out numerical simulation following the strategy presented in Sec. 3.4.

### 3.1 Outline of the method

Our calculation is based on ref. [7] to a large extent, but in order to clarify some modifications and to define quantities necessary for the discussion below, we briefly explain our calculation method. We consider the quenched QED action in Euclidean lattice, setting the lattice spacing  $a$  to  $a = 1$ , as

$$S = \frac{1}{4} \sum_{n,\mu,\nu} \left[ e^{-\nabla^2/\Lambda_{\text{UV}}^2} (\nabla_\mu A_\nu(n) - \nabla_\nu A_\mu(n)) \right]^2 + \frac{1}{2\xi} \sum_n \left[ e^{-\nabla^2/\Lambda_{\text{UV}}^2} \sum_\mu \nabla_\mu^* A_\mu(n) \right]^2 + \frac{1}{2} m_\gamma^2 \sum_{n,\mu} [e^{-\nabla^2/\Lambda_{\text{UV}}^2} A_\mu(n)]^2, \quad (3.1)$$

where

$$\nabla_\mu f(n) \equiv f(n + \hat{\mu}) - f(n), \quad \nabla_\mu^* f(n) \equiv f(n) - f(n - \hat{\mu}), \quad (3.2)$$

and  $\nabla^2 = \sum_\mu \nabla_\mu \nabla_\mu^*$ . Here we introduce a smearing parameter  $\Lambda_{\text{UV}}$ , finite photon mass  $m_\gamma$ , and a gauge fixing parameter  $\xi$  [7]. The photon two point function is exactly given in quenched QED as

$$\begin{aligned} \langle \tilde{A}_\mu(k) \tilde{A}_\nu(k') \rangle &= V \delta_{k+k',0} e^{-2\hat{k}^2/\Lambda_{\text{UV}}^2} \left[ \left( \delta_{\mu\nu} - \frac{\hat{k}_\mu \hat{k}_\nu}{\hat{k}^2} \right) \frac{1}{\hat{k}^2 + m_\gamma^2} + \frac{\hat{k}_\mu \hat{k}_\nu}{\hat{k}^2} \frac{\xi}{\hat{k}^2 + \xi m_\gamma^2} \right] \\ &\equiv V \delta_{k+k',0} \mathcal{D}_{\mu\nu}(k) \end{aligned} \quad (3.3)$$

where  $\hat{k}_\mu \equiv 2 \sin(k_\mu/2)$  and  $\hat{k}^2 = \hat{k}_\mu \hat{k}_\mu$ .  $V$  denotes the four-dimensional spacetime volume. We define the Fourier transform by  $\tilde{A}_\mu(k) = \sum_n A_\mu(n) e^{-ik(x_n + \hat{\mu}/2)}$ . There are no quantum corrections to  $\xi$ ,  $m_\gamma$ , and the normalization of the photon wave function in quenched QED. Even though we introduce non-zero photon mass, we argued [7] that similar Ward-Takahashi (WT) identities to the massless photon theory hold. We can repeat a parallel argument in the quenched QED case. Particularly we can conclude that the renormalization of the coupling constant is related to the wave function renormalization of the photon as

$$e_P = Z_3^{1/2} e. \quad (3.4)$$

As noted,  $Z_3$  can be exactly calculated at the tree-level due to the absence of the dynamical fermion.

We are interested in the  $g$ -factor, which can be extracted from the three-point function

$$\begin{aligned} G_\mu(p, k) &\equiv \frac{1}{V} \sum_{n,m,\ell} \langle (D^{-1})_{nm} A_\mu(\ell) \rangle e^{-ipx_n} e^{-i(-p-k)x_m} e^{-ik(x_\ell + \mu/2)} \\ &= \frac{1}{V} \langle \tilde{D}^{-1}(p, -p-k) \tilde{A}_\mu(k) \rangle, \end{aligned} \quad (3.5)$$

where the photon momentum is  $k$ , and the ingoing and outgoing fermion momenta are  $p$  and  $p+k$ , respectively. Here the matrix  $D$  is the covariant derivative acting to the fermion field in the nonquenched QED Lagrangian and given by

$$D_{nm} \equiv m \delta_{nm} + \frac{1}{2} \sum_\mu \left[ \gamma_\mu e^{ieA_\mu(n)} \delta_{n+\hat{\mu},m} - \gamma_\mu e^{-ieA_\mu(n-\hat{\mu})} \delta_{n-\hat{\mu},m} \right]. \quad (3.6)$$

We denote the bare electron mass by  $m$  and the on-shell mass by  $m_f$ . We define the electron propagator by

$$S(p) \equiv \frac{1}{V} \langle \tilde{D}^{-1}(p, -p) \rangle. \quad (3.7)$$

We define the vertex function  $\Gamma_\mu(p, k)$  amputating the external legs,

$$-ie_P \Gamma_\mu(p, k) = \kappa \mathcal{D}_{\mu\nu}^{-1}(k) S(p)^{-1} G_\nu(p, k) S(p+k)^{-1}, \quad (3.8)$$

where  $\kappa$  is given by a product of renormalization factors but needs not to be specified here. In continuum spacetime,  $\bar{u}(p)\Gamma_\mu(p, k)u(p+k)$  can be decomposed into two parts:

$$-ie_P \bar{u}(p)\Gamma_\mu(p, k)u(p+k) = -ie_P \bar{u}(p) \left( F_1(k^2)\gamma_\mu - F_2(k^2)\frac{\sigma_{\mu\nu}k_\nu}{2m_f} \right) u(p+k) \quad (3.9)$$

where  $\sigma_{\mu\nu} = (i/2)[\gamma_\mu, \gamma_\nu]$  and the wave function satisfies  $(-i\not{p} - m)u(p) = 0$  with  $p_0 = i\sqrt{\vec{p}^2 + m_f^2}$ . The  $g$  factor is defined by

$$\frac{g}{2} = \frac{F_1(0) + F_2(0)}{F_1(0)}. \quad (3.10)$$

To obtain the  $g$  factor in lattice, we need to compute

$$\hat{G}_\mu(p, k) \equiv \mathcal{D}_{\mu\nu}^{-1}(k) G_\nu(k, p), \quad (3.11)$$

and

$$\hat{G}_\mu^{(\text{norm})}(p, k) = -iS(p)\gamma_\mu S(p+k). \quad (3.12)$$

Although the form factors are defined for the *on-shell* fermion, we obtain these quantities for Euclidean momenta. To read off on-shell amplitudes, we consider Fourier transform of  $\hat{G}_\mu(p, k)$  and  $\hat{G}_\mu^{(\text{norm})}(p, k)$ . The formula we use is

$$\frac{g}{2} = \lim_{t \rightarrow \infty} \frac{g(t)}{2}, \quad \frac{g(t)}{2} = \frac{\mathcal{F}_M(t)/\mathcal{F}_E(t)}{\mathcal{F}_M^{(\text{norm})}(t)/\mathcal{F}_E^{(\text{norm})}(t)}, \quad (3.13)$$

where

$$\mathcal{F}_E(t) = \sum_{p_4} \text{tr}[\gamma_4 \hat{G}_4] e^{ip_4 t}, \quad (3.14)$$

$$\mathcal{F}_M(t) = \sum_{p_4} \sum_{i,j,k=1}^3 i\epsilon_{ijk} \text{tr}[\gamma_5 \gamma_i \hat{G}_j] \hat{k}_k e^{ip_4 t}, \quad (3.15)$$

and  $\mathcal{F}_E^{(\text{norm})}(t)$  and  $\mathcal{F}_M^{(\text{norm})}(t)$  are defined in a parallel manner by using  $\hat{G}^{(\text{norm})}$  instead of  $\hat{G}$ . The reason why we can obtain the  $g$  factor using this formula is explained in Sec. 6 in ref. [7]. We note that systematic uncertainties, such as discretization effects and finite photon momentum effects, are left in eq. (3.13) and should be removed.

We explain how to compute  $\hat{G}_\mu(p, k)$ . From the fact that

$$\int DA_\mu (D[A_\mu]^{-1})_{nm} e^{-S[A_\mu]} \quad (3.16)$$

is invariant under the change of the integration variable  $A_\mu(n) \rightarrow A_\mu(n) + \epsilon_\mu(n)$  (here we write  $D[A_\mu]$  to explicitly show that the covariant derivative (3.6) is a functional of  $A_\mu$ ), we obtain a Schwinger-Dyson equation,

$$-\left\langle \frac{\delta S}{\delta A_\mu(\ell)} D_{nm}^{-1} \right\rangle = \left\langle \left( D^{-1} \cdot \frac{\delta D}{\delta A_\mu(\ell)} \cdot D^{-1} \right)_{nm} \right\rangle. \quad (3.17)$$

Noting that the left-hand side is given by

$$-\sum_{k'} \frac{1}{V} e^{ik'(x_\ell + \hat{\mu}/2)} \mathcal{D}_{\mu\nu}^{-1}(k') \left\langle \tilde{A}_\nu(k') (D^{-1})_{nm} \right\rangle, \quad (3.18)$$

we obtain an identity in momentum space,

$$\hat{G}_\mu(p, k) = -\frac{1}{V} \sum_{n, m, \ell} \left\langle \left( D^{-1} \cdot \frac{\delta D}{\delta A_\mu(\ell)} \cdot D^{-1} \right)_{nm} \right\rangle e^{-ipx_n} e^{-i(-p-k)x_m} e^{-ik(x_\ell + \hat{\mu}/2)}. \quad (3.19)$$

In giving  $\hat{G}_\mu(p, k)$ , we evaluate the right-hand side, replacing  $\delta D/\delta A_\mu(\ell)$  with its  $a \rightarrow 0$  limit value. The use of eq. (3.19) significantly reduces the statistical error. The computation via Eq. (3.5) at the fixed order reduces to calculating multi-point correlation functions of photons, where the momentum conservation requires to pick up  $\tilde{A}_\mu(k)$  in the expansion of  $\tilde{D}^{-1}$ . This is done only statistically while the above formula can skip the procedure.

We evaluate eqs. (3.11) [or (3.19)] and (3.12) in perturbation theory. The perturbative formulae for  $\delta D/\delta A_\mu$  and  $D^{-1}$  are given in Sec. 2 of ref. [7]. We note that, as explained in ref. [7],  $D^{-1}$  can be evaluated fast within perturbation theory by using the fast Fourier transform. After the formal perturbative expansion of  $D^{-1}$  and  $\delta D/\delta A_\mu$ , all we have to do is to evaluate correlation functions of gauge fields,  $\langle A_{\mu_1}(n_1) A_{\mu_2}(n_2) \dots \rangle$ . Since the weight  $e^{-S[A_\mu]}$  is just a Gaussian, we generate configurations according to the Gaussian distribution to measure expectation values.

In our lattice calculations, we consider momenta,

$$p = (\vec{p}, p_4) = (-\vec{k}/2, p_4) \quad (3.20)$$

with  $k = (0, 0, 2\pi/L, 0)$  and  $(2\pi/L, 0, 2\pi/L, 0)$ . These two momenta are used for extrapolation to  $k^2 \rightarrow 0$ .  $p_4$  is summed over afterwards in eq. (3.14) etc. For this choice, the other fermion has momenta

$$p + k = (\vec{k}/2, p_4) \quad (3.21)$$

and the positions of the on-shell pole of  $S(p)$  and  $S(p+k)$  are the same.

### 3.2 Backward propagation and its suppression

The sum over  $p_4$  such as the one in eq. (3.14) gives a contribution from propagation which wraps around the torus (backward propagation). For example, let us consider

$$f_T(t) \equiv \frac{1}{T} \sum_{p_4} \frac{1}{\sin(p_4)^2 + E^2} e^{ip_4 t} = \frac{1}{T} \sum_{n=0}^{T-1} \frac{1}{\sin\left(\frac{2\pi}{T}n\right)^2 + E^2} e^{i\frac{2\pi}{T}nt}, \quad (3.22)$$

which mimics Fourier transform of a two point function, where  $E$  denotes energy. We obtain the exact formula for this sum,

$$f_T(t) = \frac{4}{\left(\frac{1}{z_*^2} - z_*^2\right)(1 - z_*^T)}(z_*^t + z_*^{T-t}) \quad (3.23)$$

for even  $t$  with  $0 \leq t < T$  and zero for odd  $t$ .  $z_*$  denotes a pole in the  $z(= e^{ip_4})$ -plane and is given by  $z_* = -E + \sqrt{1 + E^2}$ .

In eq. (3.23),  $z_*^{T-t}$  is the backward propagation. This is an obstacle in investigating large- $t$  behavior since it gradually becomes similar size to the interested contribution  $z_*^t$  for large  $t$ . This was actually an obstacle in our previous study [7].

Let us consider to take finer  $p_4$  in the sum,

$$g(t) \equiv \frac{1}{2T} \sum_n \frac{1}{\sin\left(\frac{2\pi}{T}n\right)^2 + E^2} e^{i\frac{2\pi}{T}nt} \quad (3.24)$$

with  $n = 0, 1/2, 1, 3/2, \dots$ . One can see that  $g(t) = f_{2T}(t)$ . Therefore, in this case the backward propagation is given by  $z_*^{2T-t}$  and gets milder than the previous case.

We suppress the backward propagation in our study by taking finer  $p_4$  as in the above case. We accomplish this by changing boundary conditions for the fermion [18, 19].

### 3.3 Effects of $m_\gamma$ , $k^2$ , and $\Lambda_{\text{UV}}^2$

The  $g$  factor obtained by eq. (3.13) receives discretization effects, finite volume effects, and effects of modification of Lagrangian, i.e., finite photon mass and finite  $\Lambda_{\text{UV}}^2$ , and also non-zero photon momentum  $k^2$ . (Although  $g$  factor is defined for  $k^2 \rightarrow 0$ , we consider finite  $k^2$  in our calculation.) Here we consider effects of  $m_\gamma$ ,  $k^2$  and  $\Lambda_{\text{UV}}^2$  in *continuum and infinite volume* spacetime. The FV corrections are exponentially suppressed for  $m_\gamma L \gg 1$  as discussed in Sec. 2.3. The discretization effects are discussed in the subsequent subsection.

Our consideration is given at the one-loop level. At one-loop, it is sufficient to focus only on  $F_2$  because the one-loop contribution to  $F_1$  totally vanishes in the quantity  $(F_1(k^2) + F_2(k^2))/F_1(k^2)$  due to  $F_1 = 1 + \mathcal{O}(\alpha)$  and  $F_2 = \mathcal{O}(\alpha)$ . Assuming on-shell fermion momenta  $p^2 = (p+k)^2 = -m_f^2$ , we have

$$\begin{aligned} & \bar{u}(p)\Gamma(p, k)u(p+k)|_{\text{one-loop}} \\ &= -e^2 \int \frac{d^d\ell}{(2\pi)^d} \bar{u}(p) \frac{\gamma_\rho(-i(\not{p} + \not{\ell}) + m_f)\gamma^\mu(-i(\not{p} + \not{k} + \not{\ell}) + m_f)\gamma^\rho}{[m_f^2 + (p+\ell)^2][m_f^2 + (p+k+\ell)^2][\ell^2 + m_\gamma^2]} u(p+k) \\ &= -e^2 \int_0^1 dy dz 2y \int \frac{d^4\ell}{(2\pi)^4} \bar{u}(p) \frac{4\ell \bar{p}^\mu - 4im_f \ell^\mu - 2(2-d)\ell \ell^\mu}{[\ell^2 + y\ell \cdot (\bar{p} + (1-2z)k) + (1-y)m_\gamma^2]^3} u(p+k) + (\gamma_\mu\text{-term}). \end{aligned} \quad (3.25)$$

We expressed  $p$  and  $k$  by linear combinations of  $\bar{p} \equiv (p+k) + p$  and  $k = (p+k) - p$ . They satisfy  $\bar{p} \cdot k = 0$  and  $\bar{p}^2 = -4m_f^2 - k^2$  for  $p^2 = (p+k)^2 = -m_f^2$ . After some calculation and

using the Gordon identity  $\bar{u}(p)(-i\bar{p}_\mu)u(p+k) = \bar{u}(p)(2m_f\gamma_\mu + \sigma_{\mu\nu}k_\nu)u(p+k)$ , we obtain

$$\begin{aligned}
& \bar{u}(p)\Gamma(p,k)u(p+k)|_{\text{one-loop}} \\
&= -e^2\bar{u}(p)\frac{\sigma_{\mu\nu}k_\nu}{2m_f}u(p+k)\frac{1}{(4\pi)^2}\int dydz\frac{4y^2(1-y)}{y^2+y^2z(1-z)\frac{k^2}{m_f^2}+(1-y)\frac{m_\gamma^2}{m_f^2}}+(\gamma^\mu\text{-term}) \\
&= -e^2\bar{u}(p)\frac{\sigma_{\mu\nu}k_\nu}{2m_f}u(p+k)\frac{1}{(4\pi)^2}\left(2-\frac{1}{3}\frac{k^2}{m_f^2}-2\pi\frac{m_\gamma}{m_f}+\dots\right)+(\gamma^\mu\text{-term}). \tag{3.26}
\end{aligned}$$

In the final expression, we assumed  $k^2/m_f^2 \ll 1$  and  $m_\gamma^2/m_f^2 \ll 1$ . Inside the brackets, the first term “2” gives the exact result of  $F_2(0)$ . The finite  $k^2$  and  $m_\gamma^2$  effects are found to be  $\mathcal{O}(k^2/m_f^2)$  and  $\mathcal{O}(m_\gamma/m_f)$ .

When we also turn on the UV cutoff scale  $\Lambda_{\text{UV}}$ , we have

$$\begin{aligned}
& \bar{u}(p)\Gamma(p,k)u(p+k)|_{\text{one-loop}} \\
&= -e^2\frac{1}{16\pi^2}\bar{u}(p)\frac{\sigma_{\mu\nu}k_\nu}{2m_f}u(p+k) \\
&\times \int_0^1 dydz \left[ 4y^2 \int_0^\infty ds \frac{s^3}{\left(s + \frac{2m_f^2}{\Lambda_{\text{UV}}^2}\right)^3} e^{-\frac{s^2}{2m_f^2}y^2(1+z(1-z)k^2/m_f^2)-s(1-y)m_\gamma^2/m_f^2} \right. \\
&\quad \left. - 4y^3 \int_0^\infty ds \frac{s^4}{\left(s + \frac{2m_f^2}{\Lambda_{\text{UV}}^2}\right)^4} e^{-\frac{s^2}{2m_f^2}y^2(1+z(1-z)k^2/m_f^2)-s(1-y)m_\gamma^2/m_f^2} \right] \\
&+ (\gamma^\mu\text{-term}). \tag{3.27}
\end{aligned}$$

This additionally gives a correction of  $\mathcal{O}[(2m_f^2/\Lambda_{\text{UV}}^2)\log(2m_f^2/\Lambda_{\text{UV}}^2)]$ .<sup>1</sup>

### 3.4 Calculation strategy

In this section, we discuss an optimal strategy to obtain the  $g$  factor based on the above studies. As an IR regularization, as mentioned above, we adopt photon mass regularization. We consider the following properties advantageous. (i) It is clear that the finite volume effects are exponentially suppressed, independent of the details of considered quantities. This is in contrast to the finite volume effects in QED<sub>L</sub> or QED<sub>TL</sub>, which depend on details of considered quantities such as its external momentum. (ii) Owing to (i), the IR structure of massive photon theory with finite lattice is the same as massive photon theory with infinite volume. The latter is well understood.

Adopting massive photon regularization, we first consider  $k^2 \rightarrow 0$  extrapolation. In the  $g$  factor, IR divergences appear only for  $k^2 \neq 0$  (when  $m_\gamma = 0$ ). This extrapolation therefore removes the IR divergences and makes the  $g$  factor nonsingular at  $m_\gamma = 0$ . Since

<sup>1</sup>The  $s$ -integral can be decomposed into  $\int_0^\infty ds = \int_0^1 ds + \int_1^\infty ds$ . While the integral  $\int_1^\infty ds$  gives an expansion in  $2m_f^2/\Lambda_{\text{UV}}^2$ , the integral  $\int_0^1 ds$  can give a  $2m_f^2/\Lambda_{\text{UV}}^2 \log(2m_f^2/\Lambda_{\text{UV}}^2)$  term.

we found the finite  $k^2$  effect to be  $\mathcal{O}(k^2/m_f^2)$  in the one-loop analysis, we perform linear extrapolation in  $k^2/m_f^2$ .

At this stage, we are left with finite photon mass effects and finite lattice spacing effects. We assume finite photon mass effects to be  $\mathcal{O}(m_\gamma/m_f)$  from the above study. Finite lattice spacing effects are given by  $\mathcal{O}(m_f^2 a^2)$ . We also expect finite lattice spacing effects of  $\mathcal{O}(m_\gamma a)$  because we do not find a reason to prohibit this for finite  $m_\gamma$ . In this sense, it is straightforward to perform  $m_\gamma \rightarrow 0$  extrapolation before  $m_f \rightarrow 0$  extrapolation. To summarize, we first perform linear extrapolation in  $k^2/m_f^2 \rightarrow 0$ , secondly linear extrapolation in  $m_\gamma/m_f \rightarrow 0$ , and finally linear extrapolation in  $m_f^2 a^2 \rightarrow 0$ .

Our concrete setup is as follows. For one lattice size  $L^3 \times T$ , we choose one fermion mass  $m$ . We use two different photon momenta to perform  $k^2 \rightarrow 0$  extrapolation, and also vary  $m_\gamma$  to perform  $m_\gamma/m_f \rightarrow 0$  (and  $m_\gamma a \rightarrow 0$ ) extrapolations. For a different lattice size, we choose a different fermion mass. Different lattices are used to perform  $m_f^2 a^2 \rightarrow 0$  extrapolation. (See Table 1.)

If we aim at 10 % precision lattice data (before any extrapolations) while setting

$$m_\gamma L \simeq 4 \tag{3.28}$$

in order to sufficiently suppress FV effects, we need<sup>2</sup>

$$k_{\min}^2/m_f^2, m_\gamma/m_f, m_f^2 a^2 \lesssim 0.1. \tag{3.29}$$

These conditions are satisfied with  $L \gtrsim 120$ . This large (but realistic) lattice is required for precision study.

We finally mention finite  $\Lambda_{\text{UV}}^2$  effects. In our simulation, we use a fixed value of  $\Lambda_{\text{UV}}^2 a^2$ ; see Table 1. Since we use larger fermion mass for larger lattice, finite  $\Lambda_{\text{UV}}^2$  effects,  $\sim 2m_f^2/\Lambda_{\text{UV}}^2$ , are expected to be removed simultaneously in the  $m_f^2 a^2 \rightarrow 0$  extrapolation.

### 3.5 Numerical results

We carry out lattice simulation following the strategy discussed above. However, unfortunately since we cannot use large enough lattice in the present study, we cannot keep all the systematic uncertainties under good control. We nevertheless perform lattice simulation to roughly confirm feasibility of the calculation.

We perform a numerical simulation by using small lattices listed in Table 1. For each lattice size, the smallest  $m_\gamma$  is chosen so that  $m_\gamma L = 4.0$  which makes FV effects exponentially suppressed. The fermion mass  $m$  and other values of  $m_\gamma$  are then chosen to satisfy  $m_\gamma/m = 0.4, 0.5, 0.6, 0.7$ . These points are used for taking the  $m_\gamma \rightarrow 0$  limit.

The configurations are generated according to the probability distribution  $\propto e^{-S}$  with the action in Eq. (3.1). In the momentum space, the action is diagonalized as

$$S = \frac{1}{2V} \sum_{k, \mu, \nu} \tilde{A}_\mu(k) \mathcal{D}_{\mu\nu}^{-1}(k) \tilde{A}_\nu(-k), \tag{3.30}$$

---

<sup>2</sup>We neglect  $m_\gamma a$  in this discussion.

$L^3 \times T$	$ma$	$(\Lambda_{\text{UV}}a)^2$	$\xi$	$m_\gamma a$	$N_{\text{conf}}$	extrapolation points
$14^3 \times 28$	0.714	4.0	1.0	0.2857, 0.3571, 0.4286, 0.50	780	[7:9]
$16^3 \times 32$	0.625	4.0	1.0	0.25, 0.3125, 0.375, 0.4375	780	[7:9]
$18^3 \times 36$	0.556	4.0	1.0	0.222, 0.278, 0.333, 0.389	1000	[9:11]
$20^3 \times 40$	0.50	4.0	1.0	0.20, 0.25, 0.30, 0.35	520	[9:11]
$24^3 \times 48$	0.417	4.0	1.0	0.167, 0.208, 0.25, 0.291	560	[11:13]

**Table 1.** Simulation parameters.

where  $\mathcal{D}_{\mu\nu}(k)$  is defined in Eq. (3.3) and  $\tilde{A}_\mu(-k) = \tilde{A}_\mu^*(k)$ . By choosing  $\xi = 1$ ,  $\mathcal{D}_{\mu\nu}^{-1}(k) \propto \delta_{\mu\nu}$ , and thus each component of  $\tilde{A}_\mu(k)$  has the gaussian distribution with the variance determined by  $k^2$ . The generation of the configurations can be done with almost no cost.

By using the gauge configurations, we perform the computations of the three point function in Eq. (3.19) for the smallest and the next smallest photon momenta:  $k_\mu = (0, 0, 2\pi/L, 0)$  and  $(2\pi/L, 0, 2\pi/L, 0)$ , and extrapolate to  $k^2 = 0$ . We show in Fig. 1 the perturbative expansion of the function  $g(t)/2$  in Eq. (3.13) for the case of  $m_\gamma a = 0.167$  on the  $24^3 \times 48$  lattice. Extrapolations to  $t \rightarrow \infty$  are done with the function  $g(t)/2 = a + b/t$  by using two points around  $t \sim L/2$ , *i.e.*,  $t = 11$  and 13.

We examine the stability of the extrapolation to  $t \rightarrow \infty$  by comparing with the results with other choices of the two extrapolation points. In Fig. 2, we show the perturbative coefficients obtained by the extrapolation of the points at  $t$  and  $t + 2$  with the function  $g(t)/2 = a + b/t$ . The gray bands represent our choice of  $t = 11$ . It is expected that for small  $t$  the contributions from excited states, such as a photon-electron two particle state, in the integrations in Eqs. (3.14) and (3.15) cannot be ignored. On the other hand, for large  $t$  the finite volume effects are important. The effects of the backward propagation of the fermion are enhanced for higher orders in perturbation, as the expansion the fermion pole mass,  $m_f$ , in the backward propagation factor,  $e^{-m_f(T-t)}$ , gives large coefficients for higher orders. As discussed in Sec 3.2, we used both the periodic and anti-periodic boundary conditions of fermions to evaluate three-point functions at the fermion Euclidean energies  $p_4 = 0, \pi/T, 2\pi/T, \dots$ . This treatment effectively enlarges the extent in the time direction  $T$  to  $2T$ . The backward propagation is significantly suppressed, but still it is better to be away from a large  $t$  region. The choice of  $t \sim L/2$  seems to give a reasonably stable values although it is desired to have larger statistics for the confirmation of the stability for three loops and higher.

Obtained values of  $g(t \rightarrow \infty)/2$  are plotted for four choices of  $m_\gamma a$  in Fig. 3. Three points  $m_\gamma/m = 0.4, 0.5, 0.6$  are used for the linear extrapolation to  $m_\gamma = 0$  while fixing  $m$ . Expected systematic uncertainties by this extrapolation, are of order 20–30% due to higher order terms in the  $m_\gamma$  expansion, *i.e.*,  $\mathcal{O}(m_\gamma^2/m_f^2)$ . The effects of the discretization are expected to be larger for higher orders in perturbations. In addition to the discretization effects of  $\mathcal{O}(m^2 a^2)$ , the UV cut-off in the photon kinetic term gives corrections typically,

$$e^{-2m^2/\Lambda^2}, \quad (3.31)$$

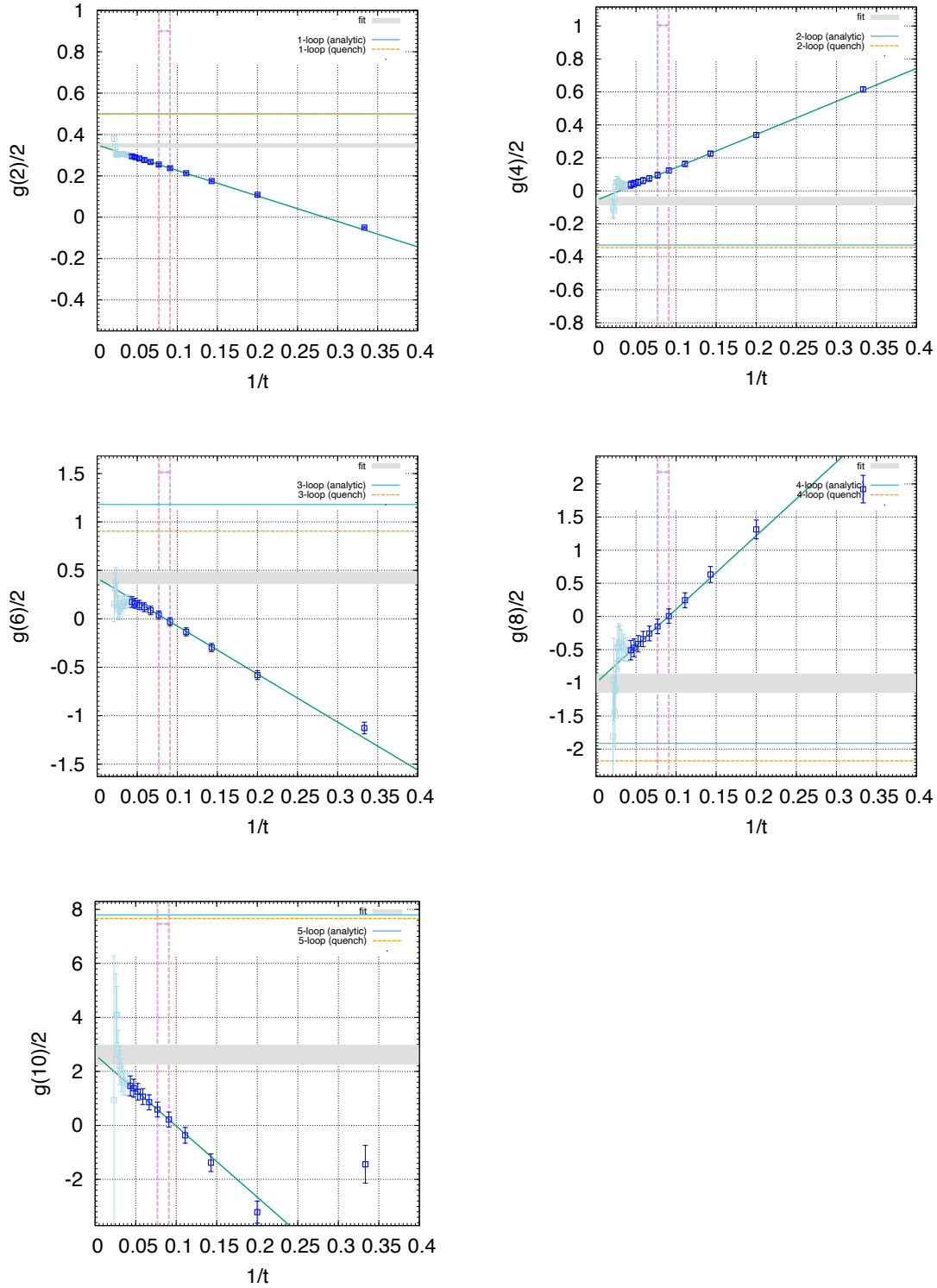


**Figure 1.** The perturbative coefficients of the function  $g(t)/2$  on the  $24^3 \times 48$  lattice. The photon mass is  $m_\gamma a = 0.167$ . Other parameters are listed in Table 1.

as a multiplicative factor for each photon propagator. For a choice of too small  $\Lambda/m$ , we

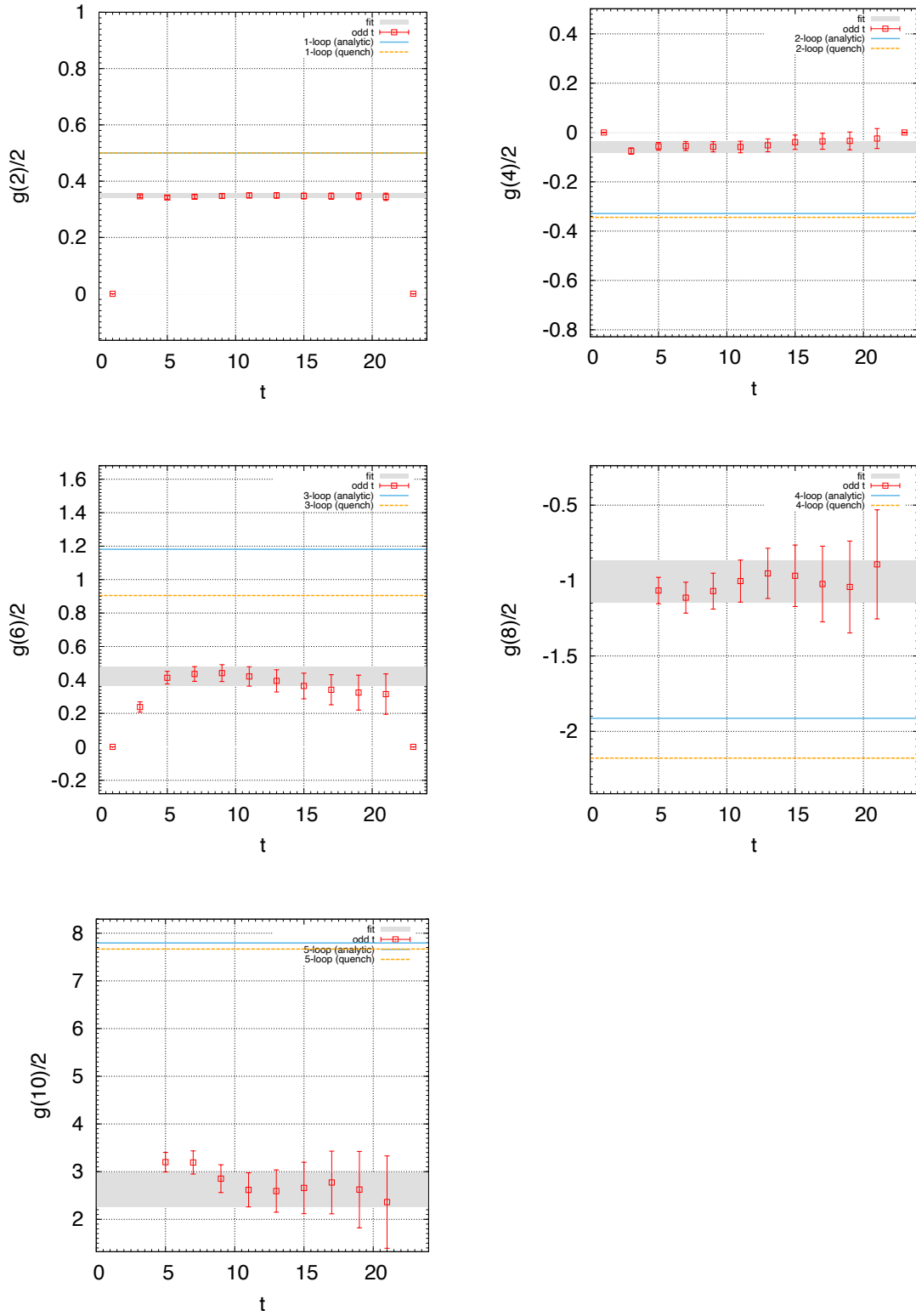


**Figure 2.** The stability of the extrapolation to  $t \rightarrow \infty$ .

obtain exponentially suppressed values. The choice of  $\Lambda^2 = 4.0$  seems to be not too small. Further large values, however, make the statistical error larger and also the logarithmic correction larger. One should look for optimal values of  $\Lambda$  for different choices of simulation parameters.

We show the analytic results of  $g/2$  with finite photon masses at the one-loop level (using the first equality of eq. (3.26) with  $k^2 = 0$ ) in Fig. 3 as the solid curve. The lattice results are significantly off the line, which represents the discretization effects. With the finite photon mass, there can be discretization errors of order  $m_\gamma a$  in addition to  $m^2 a^2$ . Therefore, the limit of  $m_\gamma \rightarrow 0$  would give the closest value to the continuum theory. Such a tendency can be seen in the figure.

We repeat the same analyses for  $L = 20, 18, 16$  and  $14$ , while keeping  $m_\gamma/m = 0.4-0.7$  and  $m_\gamma L = 4$  for the smallest  $m_\gamma$  as listed in Table 1. For smaller lattices, the fermion mass  $ma$  is larger, and thus results are further from the continuum limit. We show in Fig. 4 the  $m^2 a^2$  dependence of the  $g$  factor on each lattice. We see the tendency of approaching towards the correct values.

Although the statistical uncertainties are large, the calculation up to the five-loop level seems to be doable in a larger scale simulation. For  $L = 128$ , for example, one can take  $m_\gamma/m = 0.1$  and  $m^2 a^2 = 0.1$  while satisfying  $m_\gamma L = 4$ . This would significantly reduce the uncertainties of the  $m_\gamma \rightarrow 0$  extrapolation.

## 4 Conclusions and discussion

In this paper, aiming at giving the five-loop coefficient of the electron  $g$  factor using lattice, we developed theoretical study of finite volume corrections and also performed a numerical simulation using small lattices. We first studied finite volume corrections in various IR regularization methods of lattice QED to discuss optimal regularization for our purpose. We found that, in  $\text{QED}_L$  and in  $\text{QED}_{TL}$ , finite volume corrections are sensitive to external momentum of a correlation function; they differ for Euclidean momentum and for on-shell momentum. Therefore the previous study [16] which sets the external momentum to on-shell from the beginning gave an incorrect result. In our study to obtain the  $g$  factor, we need to make two components of the external momentum non-zero and need an extension of  $\text{QED}_L$ , which is considered for one non-zero component of the external momentum. In this case the finite volume corrections get severer. In contrast to the complexity of finite volume effects in  $\text{QED}_L$  as mentioned above, finite photon mass regularization seems to always suppress finite volume corrections exponentially  $\sim e^{-m_\gamma L}$ . We therefore adopt finite photon mass regularization.

In addition to finite volume effects, we studied corrections to the  $g$  factor due to finite photon mass and finite photon momentum  $k^2$ . We gave parameteric dependence on these perturbations; this understanding is used to fix extrapolation functions. Based on these studies on systematic errors, we presented an optimal strategy about choices of simulation parameters  $m_\gamma, m, \Lambda_{\text{UV}}^2, L$  and the order of various extrapolations.

We presented a numerical lattice simulation following our strategy. We used small lattices and the systematic uncertainties in the extrapolations we performed require more

study. With our choice of parameters, we observed large discretization effects. This can be understood from discretization effects of  $\mathcal{O}(m_\gamma a)$ ; we could not take small enough  $m_\gamma$  due to smallness of lattices. Apart from this, we observed good tendencies. First, we observed clear linear dependence in  $1/t$  for  $g(t)$  (see Figs. 1 and 2). This behavior can be understood as a consequence of suppression of backward propagation and suppression of finite volume corrections (owing to  $m_\gamma L \gg 1$ ). When finite volume corrections are not suppressed enough, higher poles appear in Fourier transformed quantities and disturb linear  $t$  dependence as discussed in ref. [7]. Secondly, we observed that the  $g$  factor has almost linear dependence in  $(ma)^2$  as expected (see Fig. 4).

The photon mass can be taken small when large lattices are available and discretization effects are expected to be much better. We estimated that the required size is  $L \sim 128$ . We would like to update our results using larger lattice in the future.

## Acknowledgements

The authors would like to thank Masashi Hayakawa for discussions. The work is supported by JSPS KAKENHI Grant Numbers JP19H00689 (RK), JP19K14711 (HT), JP21H01086 (RK) and MEXT KAKENHI Grant Number JP18H05542 (RK, HT).

## References

- [1] T. Aoyama, M. Hayakawa, T. Kinoshita, and M. Nio, “Complete Tenth-Order QED Contribution to the Muon  $g-2$ ,” *Phys. Rev. Lett.* **109** (2012) 111808, [arXiv:1205.5370 \[hep-ph\]](#).
- [2] S. Volkov, “Calculating the five-loop QED contribution to the electron anomalous magnetic moment: Graphs without lepton loops,” *Phys. Rev. D* **100** no. 9, (2019) 096004, [arXiv:1909.08015 \[hep-ph\]](#).
- [3] T. Aoyama, T. Kinoshita, and M. Nio, “Revised and Improved Value of the QED Tenth-Order Electron Anomalous Magnetic Moment,” *Phys. Rev. D* **97** no. 3, (2018) 036001, [arXiv:1712.06060 \[hep-ph\]](#).
- [4] D. Hanneke, S. Fogwell, and G. Gabrielse, “New measurement of the electron magnetic moment and the fine structure constant,” *Physical Review Letters* **100** no. 12, (Mar, 2008) . <http://dx.doi.org/10.1103/PhysRevLett.100.120801>.
- [5] X. Fan, T. G. Myers, B. A. D. Sukra, and G. Gabrielse, “Measurement of the Electron Magnetic Moment,” [arXiv:2209.13084 \[physics.atom-ph\]](#).
- [6] L. Morel, Z. Yao, P. Cladé, and S. Guellati-Khélifa, “Determination of the fine-structure constant with an accuracy of 81 parts per trillion,” *Nature* **588** no. 7836, (2020) 61–65.
- [7] R. Kitano, H. Takaura, and S. Hashimoto, “Stochastic computation of  $g - 2$  in QED,” *JHEP* **05** (2021) 199, [arXiv:2103.10106 \[hep-lat\]](#).
- [8] F. Di Renzo, G. Marchesini, P. Marenzoni, and E. Onofri, “Lattice perturbation theory on the computer,” *Nucl. Phys. B Proc. Suppl.* **34** (1994) 795–798.
- [9] F. Di Renzo, E. Onofri, G. Marchesini, and P. Marenzoni, “Four loop result in SU(3) lattice gauge theory by a stochastic method: Lattice correction to the condensate,” *Nucl. Phys. B* **426** (1994) 675–685, [arXiv:hep-lat/9405019](#).

- [10] F. Di Renzo and L. Scorzato, “Fermionic loops in numerical stochastic perturbation theory,” *Nucl. Phys. B Proc. Suppl.* **94** (2001) 567–570, [arXiv:hep-lat/0010064](#).
- [11] F. Di Renzo, V. Miccio, and L. Scorzato, “Unquenched numerical stochastic perturbation theory,” *Nucl. Phys. B Proc. Suppl.* **119** (2003) 1003–1005, [arXiv:hep-lat/0209018](#).
- [12] F. Di Renzo and L. Scorzato, “Numerical stochastic perturbation theory for full QCD,” *JHEP* **10** (2004) 073, [arXiv:hep-lat/0410010](#).
- [13] M. Hayakawa and S. Uno, “QED in finite volume and finite size scaling effect on electromagnetic properties of hadrons,” *Prog. Theor. Phys.* **120** (2008) 413–441, [arXiv:0804.2044 \[hep-ph\]](#).
- [14] Z. Davoudi, J. Harrison, A. Jüttner, A. Portelli, and M. J. Savage, “Theoretical aspects of quantum electrodynamics in a finite volume with periodic boundary conditions,” *Phys. Rev. D* **99** no. 3, (2019) 034510, [arXiv:1810.05923 \[hep-lat\]](#).
- [15] M. G. Endres, A. Shindler, B. C. Tiburzi, and A. Walker-Loud, “Massive photons: an infrared regularization scheme for lattice QCD+QED,” *Phys. Rev. Lett.* **117** no. 7, (2016) 072002, [arXiv:1507.08916 \[hep-lat\]](#).
- [16] S. Borsanyi *et al.*, “Ab initio calculation of the neutron-proton mass difference,” *Science* **347** (2015) 1452–1455, [arXiv:1406.4088 \[hep-lat\]](#).
- [17] T. Aoyama, T. Kinoshita, and M. Nio, “Theory of the Anomalous Magnetic Moment of the Electron,” *Atoms* **7** no. 1, (2019) 28.
- [18] P. F. Bedaque, “Aharonov-Bohm effect and nucleon nucleon phase shifts on the lattice,” *Phys. Lett. B* **593** (2004) 82–88, [arXiv:nucl-th/0402051](#).
- [19] L. Del Debbio, F. Di Renzo, and G. Filaci, “Large-order NSPT for lattice gauge theories with fermions: the plaquette in massless QCD,” *Eur. Phys. J. C* **78** no. 11, (2018) 974, [arXiv:1807.09518 \[hep-lat\]](#).

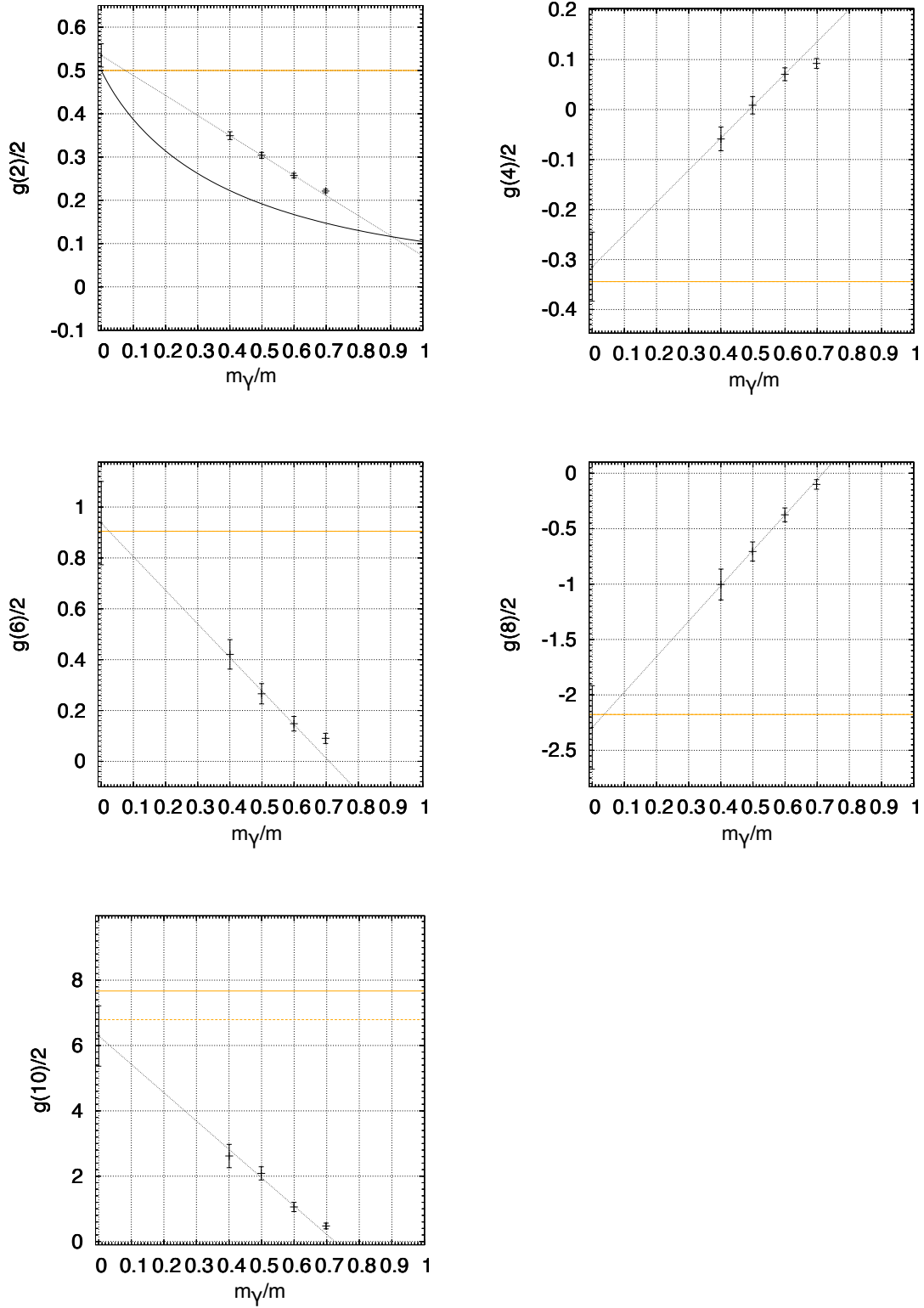


**Figure 3.** Extrapolation to  $m_\gamma = 0$ . Horizontal lines show the results from Feynman diagram computations. For the five-loop coefficient, the solid line shows the result of refs. [3, 17] while the dashed one the result of ref. [2].

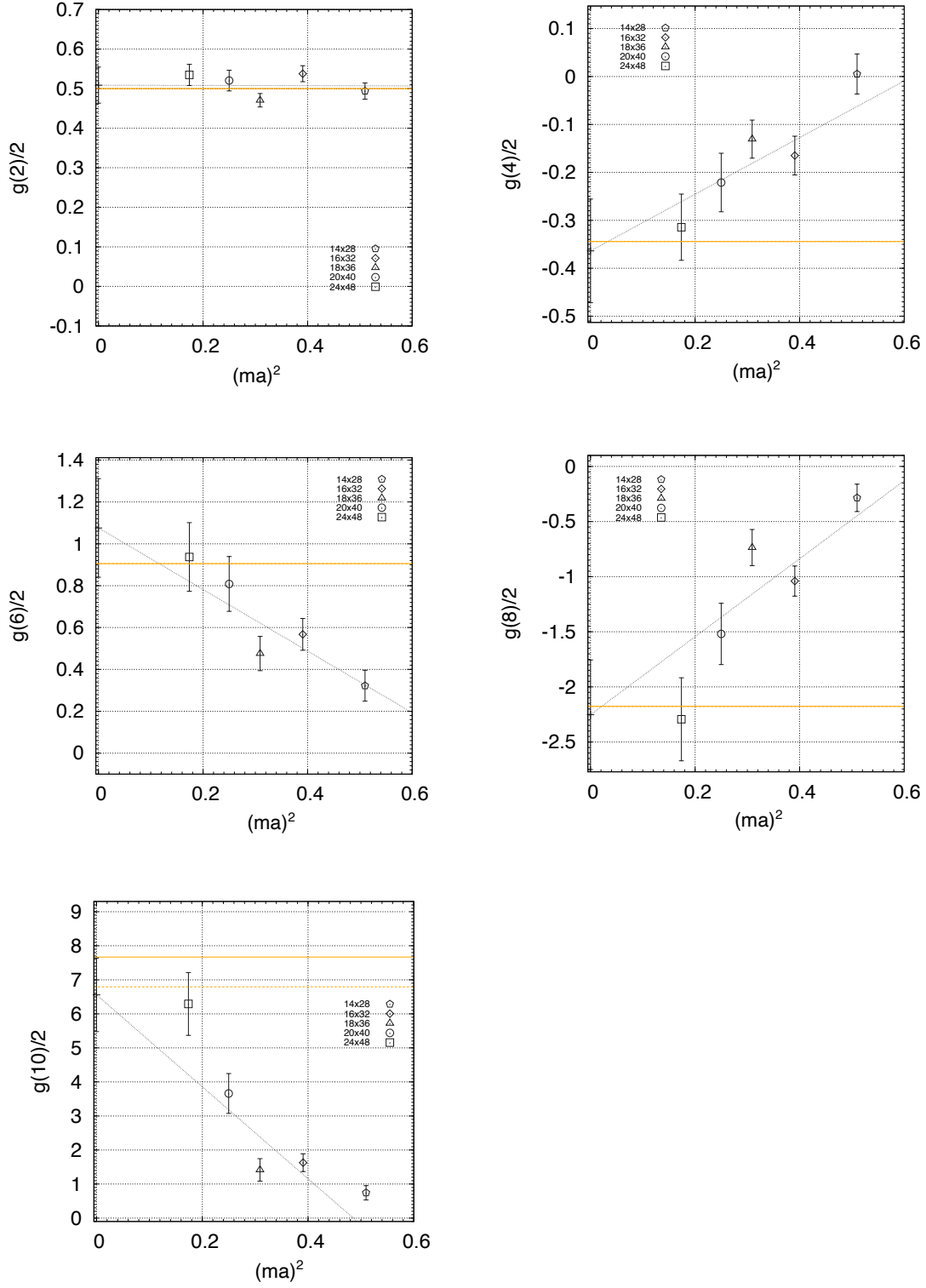


**Figure 4.** The continuum limit. For the five-loop coefficient, the solid line shows the result of refs. [3, 17] while the dashed one the result of ref. [2].